Effects of carbon on Fe-grain-boundary cohesion: First-principles determination

Ruqian Wu
Department of Physics and Astronomy, California State University, Northridge, California 91330-8268

A. J. Freeman
Department of Physics and Astronomy, Northwestern University, Evanston, Illinois 60208

G. B. Olson
Department of Materials Science and Engineering, Northwestern University, Evanston, Illinois 60208
(Received 16 August 1995)

The cohesive properties of the C/FeΣ3(111) grain boundary are investigated by means of the direct determination of the difference in binding energies of C in grain-boundary and free-surface environments. The atomic force approach based on the full-potential linearized augmented plane-wave method is used to optimize the atomic structure for the clean and C-segregated grain-boundary and free-surface systems. The ω phase structure obtained in a previous grain-boundary cluster calculation is found to be only a metastable state that is 0.72 eV/cell (0.81 J/m^2) higher in energy than the distorted bcc ground state. The calculated binding-energy difference (i.e., $\Delta E_b - \Delta E_s$) is -0.61 eV/adatom, which is a theoretical demonstration that C is a cohesion enhancer in the Fe grain boundary. Comparisons with earlier results obtained for B, S, and P show that the number of hybridized p electrons and the resulting spatial anisotropy of bonding with the surrounding Fe atoms is the key factor determining the relative embrittling or cohesion enhancing behavior of a metalloid impurity.

I. INTRODUCTION

Maintaining resistance to brittle intergranular fracture is a crucial issue as structural steels move to progressively higher strength levels.[1] The effects of the intergranular segregation of various metalloid impurities, such as P and S on the cohesive properties of an Fe grain boundary (GB), are known to play a key role. A thermodynamic theory developed by Rice and Wang[2,3] describes the mechanism of metalloid induced intergranular embrittlement through the competition between plastic crack blunting and brittle boundary separation. Their most striking result is the prediction that the potency of a segregating solute in reducing the ''Griffith work'' of brittle boundary separation is a linear function of the difference in segregation energies for that solute at the GB, ΔE_b, and at the free surface (FS), ΔE_s. Simply put, a solute with positive energy difference $\Delta E_b - \Delta E_s$ (i.e., ΔE_b is less negative) will be a more potent embrittler, while a solute with a negative difference can enhance boundary cohesion.[1,3]

Thus, a predictive theory for the intergranular cohesive properties can be established by directly determining both ΔE_b and ΔE_s, using present state-of-the-art first-principles local density electronic structure approaches. However, since $\Delta E_b - \Delta E_s$ is small (e.g., 0.4 eV per P atom for the P/Fe system),[1] (i) the GB and FS systems must be treated on an equal footing and (ii) the atomic structures of both FS and GB should be well optimized for the cases with and without the impurity atoms. The second point is extremely important for the FeΣ3(111) GB,[4] a well-studied prototypical grain boundary for investigation of the cohesive properties of steels, because there is a large stress built up in the core region of the GB. Following pioneering work using either cluster or energy band methods,[5–7] we have carried out[8–10] a series of calculations to investigate the effects of P and B impurities in the FeΣ3(111) GB and on the corresponding Fe(111) FS, with the full-potential linearized augmented plane-wave (FLAPW) approach.[11] Large unit cells in a slab model[9] containing 24 atoms for the GB and 15 atoms for the FS, were used for the sake of realistic simulation and internally consistent treatments. At that time, the task of structural optimization overwhelmed the FLAPW total energy capability, so that equilibrium geometries of the GB systems were determined using the DMol cluster method with an atomic force approach.[12] Significant results found included (i) structural relaxation may reduce the total energy of the clean Fe GB drastically by 1.61 eV/cell, which in turn affects the final value of ΔE_b; (ii) the spatial anisotropy of the impurity-Fe bonds plays a significant role for the embrittlement behavior and; (iii) while the impurities do attract charge from the surrounding Fe atoms and thus reduce the Fe-Fe bonding across the GB, this appears not to be the major reason for the impurity-induced embrittlement, as previously proposed.[5]

Unfortunately, the boundary effects in the DMol cluster calculation are still very strong even when the cluster consists of 93 atoms. Therefore, the calculated free energy difference $\Delta E_b - \Delta E_s$ may contain some significant error. Very recently, we made a breakthrough in developing a method and a code to evaluate atomic forces based on the thin film FLAPW algorithm.[13] As a result, we can now optimize the positions of all the atoms in a unit cell very efficiently and precisely (with a much weaker influence from artificial boundaries).

In this paper, we apply the FLAPW force approach to investigate the influence of segregated C on the FeΣ3(111) GB. As experimental evidence indicates that C is a GB cohesion enhancer in Fe (Refs. 1–3), the results offer insights

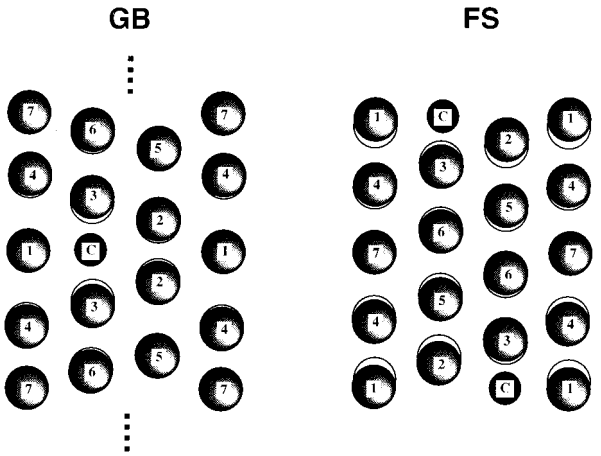

FIG. 1. Model and notation for the structure of Fe and C impurity at (left) Fe $\Sigma 3[\bar{1}10]$ (111) grain boundary, and (right) Fe(111) free surface. Open and shaded circles denote the positions of Fe atoms before and after the presence of the C impurity.

into the key electronic features underlying the influence of segregants on the boundary cohesion. Following the presentation of the model and computational details in Sec. II, we discuss the results of structural optimizations in Sec. III. The chemical and magnetic interactions, and finally the calculated free energy difference and the corresponding mechanism for the cohesive behavior, are discussed in Secs. IV, V, and VI, respectively.

II. MODEL AND COMPUTATION

As sketched in Fig.1, both the C/Fe(111) FS and C/Fe GB are simulated by a slab model,[10] which minimizes GB interactions inherent in superlattice cells.[7,8] For the C/Fe(111) FS system, the Fe(111) substrate is simulated by a 13 layer slab, and the C adatoms are placed pseudomorphically on the threefold hollow sites on both sides of the Fe slab. For the GB system, a 23 layer slab is adopted to simulate the clean Fe GB. With 12 Fe layers in between, the possible interactions between the free surface (introduced artificially in the slab model) and the GB are expected to be sufficiently reduced. The two-dimensional (2D) lattice constant and the unrelaxed Fe-Fe interatomic distance are chosen from experimental values for bulk bcc Fe, i.e., $d_{\text{Fe-Fe}}=4.69$ a.u. The slab models are sufficiently thick to allow multilayer atomic relaxation for Fe in both FS and GB environments.

In the FLAPW method,[11] no shape approximations are made for charge density, potential, and matrix elements. The core states are treated fully relativistically and the valence states are treated semirelativistically (i.e., without spin-orbit coupling).[14] We employ the Hedin and Lundqvist and the von Barth−Hedin formulas for the exchange-correlation potentials for the nonmagnetic and the spin-polarized calculations,[15] respectively. This approach has been applied very successfully in the past decade to determine the electronic and magnetic properties of many transition metal systems.[16]

Energy cutoffs of 13 Ry and 100 Ry are employed for plane-wave bases and star functions to describe the wave functions and the charge density and potential in the interstitial region, respectively. Within the muffin-tin (MT) spheres ($r_{\text{MT,Fe}}=2.1$ a.u., $r_{\text{MT,C}}=1.0$ a.u.), lattice harmonics with angular-momentum l up to 8 are adopted. Convergence is assumed when the average root-mean-square difference between the input and output charge and spin densities is less than 1×10^{-4} e/(a.u.)^3. The step-forward approach[17] is used to speed up the calculations.

TABLE I. Calculated interlayer distance starting from the grain-boundary region (in a.u.). The small negative value of d_{23} (d_{56}) means that Fe(2) (Fe(5)) and Fe(3) (Fe(6)) are almost coplanar (ω phase) but Fe(3) (Fe(6)) is slightly lower.

	Clean Fe GB			C/Fe GB	
Layer	DMol[a]	EAM[b]	FLAPW	EAM[b]	FLAPW
d_{12}	2.36	2.17	2.10	2.37	2.15
d_{23}	−0.04	0.76	1.27	1.48	1.40
d_{34}	2.37	1.89	1.50	1.34	1.40
d_{45}	2.34	1.70	1.61	1.75	1.56
d_{56}	−0.02	1.36	1.52	1.53	1.55
d_{67}	2.37	1.65	1.48	1.52	1.44

[a]Reference 12.
[b]Reference 18.

III. ATOMIC STRUCTURE

Since a well optimized atomic geometry is a prerequisite to obtain reliable electronic properties, we carried out atomic force[13] calculations to determine atomic structures (i.e., multilayer relaxation) of the clean Fe(111) surface, the clean Fe grain boundary, C/Fe(111) FS, and C/FeΣ3(111) GB.

A. The clean Fe GB

As a crucial reference system, it is very important to obtain highly precise results for the total energy, atomic structure, and bonding properties of the clean Fe GB. As stated above, we employed the DMol method (with atomic forces) to optimize the atomic structure for the Fe the GB (Ref. 12) in our previous publications.[9,10] Unfortunately, the boundary effects (or in other words the artificial stress) remain very strong in the core region of the GB even with a large cluster containing 93 atoms; thus, the reliability of the structure optimized through DMol calculations needs to be verified.

In the 24 layer slab model, we fixed the three outermost Fe layer spacings and adjusted vertical positions of all the other layers according to the calculated atomic forces. For the equlibrium structure, for which all the force on each atom becomes almost zero ($<$ 3 mRy/a.u.) and thus the total energy reaches its minimum, the calculated atomic positions are listed in Table I (also shown graphically by the open circles in Fig. 1). Results obtained through DMol and semiempirical embedded-atom[18] calculations for the Fe GB are also listed for comparison. Most strikingly, the ω phase found in the previous DMol calculations[12] is no longer the ground state, but remains as a metastable state for the clean Fe GB. It is about 0.72 eV/cell (0.81 J/m^2) higher in energy than the ground state which, as shown in Table I, is a distorted-bcc structure. Surprisingly, the structure obtained

TABLE II. Calculated interlayer distance starting from the surface (in a.u.), compared with experiment.

	Fe(111)		C/Fe(111)
Layer	Expt.[a]	Theo.	Theo.
d_{C-3}			3.42
d_{12}	1.30	1.40	1.58
d_{23}	1.41	1.22	2.00
d_{34}	1.62	1.60	1.30
d_{45}	1.52	1.51	1.45
d_{56}	1.56	1.40	1.69
d_{67}	1.56	1.52	1.43

[a]Reference 20.

from a semiempirical Finnis-Sinclair embedded atom method[18] (EAM) is very close to that obtained with the highly precise FLAPW method. For example, the free volume of the core region of the GB (first four layers) obtained through the two method are almost the same (within 1%). This means that the effect of the imposed stress from the cluster boundary contributes greater inaccuracy than that from the approximate description of the charge density and potential, etc. Therefore, one should be careful in determining the structure of a grain boundary with the cluster methods.

B. The clean Fe(111) surface

For the clean Fe(111) surface, our previous total energy calculations found[19] that the relaxation of the surface layer amounts to 0.38 a.u. and, furthermore, the multilayer relaxation [with a structure measured through low-energy electron diffraction (Ref. 20)] was found to reduce the surface energy by 0.075 eV/cell (0.084 J/m^2). Here, we reoptimized the atomic structure of the clean Fe(111) surface with the FLAPW atomic force approach, and the calculated results are listed in Table II (also shown graphically by the open circles in Fig. 1).

In general, the calculated interlayer distances appear to be about 3% smaller than experiment (note that the lattice constant in the lateral plane adopts the experimental value for bcc Fe bulk, which is about 3% larger than that obtained through the local-density approximation calculations[21]). Very interestingly, the Fe(2) plane appears to undergo the largest downward relaxation, since d_{23} (1.22 a.u.) is even smaller than d_{12} (1.40 a.u.). Subsequently, d_{56} is also smaller than d_{45} (1.40 a.u. versus 1.51 a.u.). This unusual relaxation on the rough surface deserves experimental scrutiny, and we are investigating its driving force. We found that the theoretically optimized structure is about 0.08 eV (0.09 J/m^2) lower in total energy than that obtained using the measured geometry.

C. C/Fe GB and C/Fe(111)

Since the size of the C atom is small, it can be easily acommodated in the hollow site between Fe(3) atoms across the Fe GB without interference with the surroundings. As listed in Table I and also as shown in Fig. 1 by the shaded circles, while the Fe(3) atoms are pushed by 0.18 a.u. apart from the central plane, other atoms adjust their positions only slightly (around 0.05 a.u.) relative to the clean Fe GB. By contrast, results obtained from the EAM calculations[18] indicated a long-ranged effect of the C impurity on the atomic structure in the Fe GB; even their positions of the Fe(6) and Fe(7) atoms were affected by as much as about 0.5 a.u. Thus, it appears to be important to describe the electron density self-consistently when impurity atoms are present, since significant charge redistribution is usually involved.

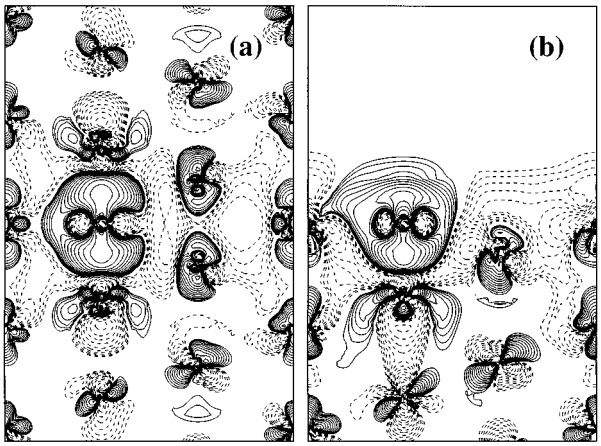

FIG. 2. The calculated valence charge density difference for (a) C/Fe GB and (b) C/Fe(111). Contours start from 5×10^{-4} e/a.u.^{3} and increase successively by a factor of $\sqrt{2}$. Solid contours denote charge accumulation and dashed lines denote charge depletion.

As found previously,[9] the bond length is shorter in the FS environment than in the GB; the calculated $d_{\text{C-Fe(3)}}$ in C/Fe(111) is 3.41 a.u.—about 4% shorter than that in the GB environment. As also found for P/Fe(111) and B/Fe(111),[22] the adsorption of C on Fe(111) induces a strong multilayer relaxation in the substrate. Comparing the positions of Fe atoms on the clean Fe(111) surface (cf. shifts between the open and shaded circles in Fig. 1), significant C-induced changes can be found for the surface [Fe(1), $\Delta z=0.50$ a.u.] and the subsurface [Fe(2), $\Delta z=0.62$ a.u.] layers. Strong effects (about 0.10 a.u.) can be found even for Fe(5) and Fe(6) layers—indicating a long-ranged effect of C on the Fe(111) FS.

IV. CHEMICAL INTERACTION

In modern first principles calculations, the charge density is a key quantity for discussion of interatomic interactions. In Fig. 2, the charge density differences, obtained by subtracting the superimposed charge density from a free C monolayer and a clean Fe GB or Fe(111) surface from the self-consistent charge density for the corresponding C/Fe system, are presented for the C/Fe GB (in panel a) and C/Fe(111) surface (in panel b), respectively. Pronounced charge redistributions can be seen clearly for both environments—indicating strong chemical interactions between C and the surrounding Fe atoms. In the GB case, very similar to the B/Fe system, the charge accumulates between C and Fe atoms and the shape of the contours suggests that the C-Fe(3) bonding is mainly via hybridization between the C-p_z and Fe(3)-d_{z^2} states. Since C has two $2p$ electrons, they should

occupy the bonding $p_{x,y}$ states and leave the nonbonding p_z state empty in the isolated C monolayer. In the C/Fe GB, however, the C-p_z state becomes lower in energy by hybridizing with the Fe(3)-d_{z^2} state and thus, as shown in Fig. 2(a), there is charge transfer from the in-plane $p_{x,y}$ states to the vertical p_z state around the C site. Therefore, C-Fe bonding shows spatial anisotropy, i.e., stronger vertical C-Fe(3) bonding and weaker lateral C-Fe(1) bonding. A very similar behavior was also found for B/Fe; however, the in-plane C-Fe(1) bonding is stronger than that between B-Fe(1), because C has one more $2p$ electron to fill more states originating from C-$p_{x,y}$.

On the C/Fe(111) surface, as shown in Fig. 2(b), a very similar C-Fe(3) bonding is found under the bottom half of the C. Since one of the Fe(3) atoms is missing in the FS system, most of the electrons on top of the C layer now occupy the in-plane states and thus the C/Fe bonding is more isotropic compared to the strong dangling bond on B/Fe(111).[10] As a result, the charge accumulation between C/Fe(1) becomes obviously stronger in the FS than in the GB. Therefore, we expect that the loss of free energy due to one broken C-Fe(3) bond can be compensated for partially through the enhanced C/Fe(1) and C-Fe(3) interaction (due to the shortened bond length). Charge depletion from the interstitial region between Fe atoms [especially between Fe(2)] can be found in both panels. Since this was also found in B/Fe and P/Fe,[10] it appears not to be an essential feature of embrittlement behavior, as believed previously.[5]

The calculated densities of states (DOS) for the C/Fe GB and C/Fe(111) FS are presented in Fig. 3. In the GB environment, the hybridization between C-$2p$ and Fe(3)-$3d$ is obvious, because resonant features can be found below -4 eV on their projected DOS curves. By contrast, the interaction between C and Fe(1) and Fe(2) appears to be weaker. However, one should keep in mind that the DOS curves are calculated only for the muffin-tin region and, as seen in Fig. 2, the main feature of the C-Fe interaction occurs in the interstitial region. On the Fe(111) surface, the C-Fe(3) hybridization is obviously much stronger than that in the GB environment, since the C-$2p$ smears over a wide energy range above -6.5 eV. Interestingly, an exchange splitting of 0.5 eV can be found for the C-$2s$ state in the C/Fe GB, while in the FS environment, this exchange splitting is almost zero. This interesting phenomenon provides one way for experimentalists to verify our theoretical results.

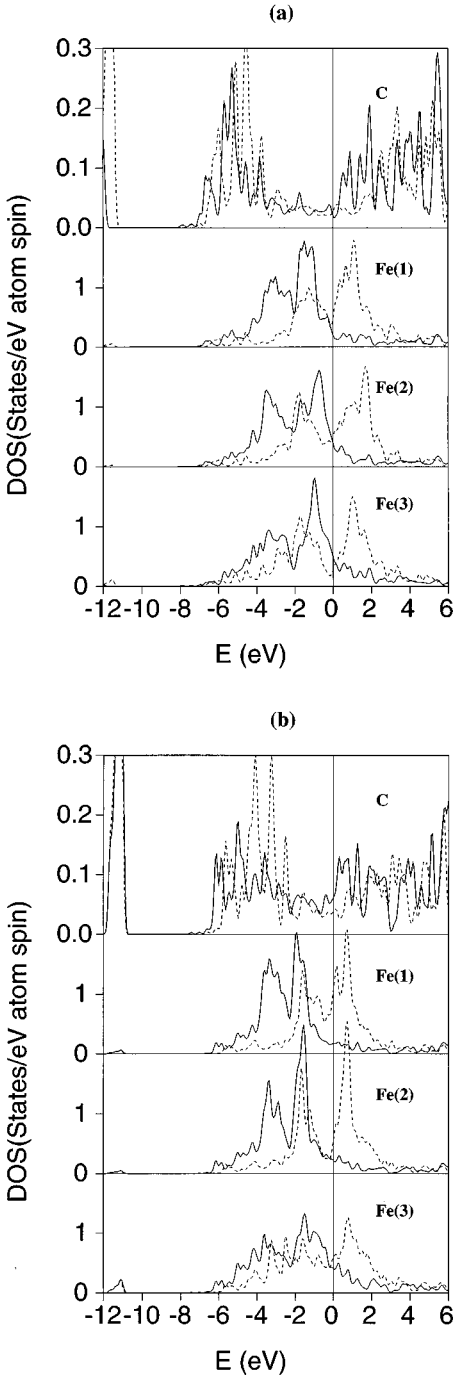

FIG. 3. The calculated density of states (DOS) for (a) C/Fe GB and (b) C/Fe(111) FS. Solid lines stand for majority spin and dashed lines represent minority spin.

V. MAGNETIC INTERACTION

The spin density difference contours for the C/Fe GB and C/Fe(111) FS are shown in Fig. 4. As revealed in the previous calculations,[8,10] the detrimental effects of the C atom on the magnetization around the Fe(1) and Fe(3) atoms are very clear and meanwhile, the magnetization around the second-rank Fe atoms is somewhat enhanced. A major difference between C and P (Ref. 10) is that the magnetization around Fe(2) undergoes enhancement in the C/Fe system. This is most probably due to the small size of the C atom, which does not directly hybridize with the Fe(2) atom. Obviously, the magnetic interaction between metalloid and the surrounding Fe atoms is long ranged and is also very sensitive to the environment. On the FS system, when the C/Fe(2) bond length is shortened by only 7%, the C-induced enhancement of magnetization around Fe(2) seen in Fig. 4(a) is completely removed.

Quantitatively, the calculated magnetic moment in each Fe muffin-tin sphere is presented in Table III. Referring to the unrelaxed GB configuration (GB1) corresponding to Fig. 4, the effects of C are obvious since they reduce the magnetic moment of Fe(3) and Fe(1) by $0.62\mu_B$ and $0.29\mu_B$, respectively. By contrast, C-induced enhancement is remarkable for the magnetic moments of Fe(2) (by $0.28\mu_B$), Fe(4) (by $0.25\mu_B$) and even for the Fe(6) (by $0.19\mu_B$). At the FS, the

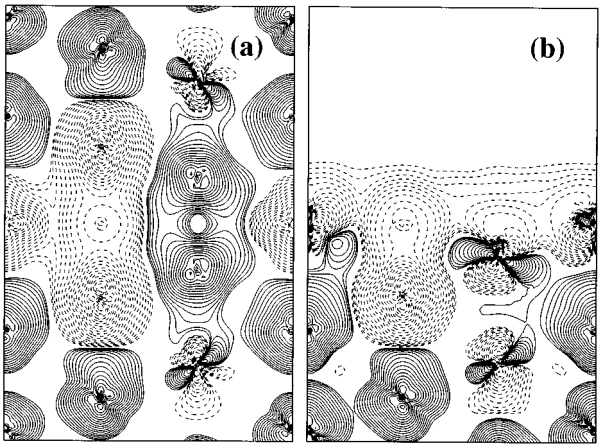

FIG. 4. The calculated spin density difference for (a) C/Fe GB and (b) C/Fe(111). Contours start from 5×10^{-4} e/a.u.^{3} and increase successively by a factor of $\sqrt{2}$. Solid contours denote spin accumulation and dashed lines denote spin depletion.

reduction of the Fe(3) magnetic moment is as large as $0.63\mu_B$. In both environments, an induced magnetic moment of $-0.04\mu_B$ is found in the muffin-tin sphere of C.

VI. SEGREGATION ENERGY AND DISCUSSION

The embrittlement behavior of C in the FeΣ3(111) GB can be determined according to the Rice-Wang model[3] through the value and sign of $\Delta E_b-\Delta E_s$. The calculated bonding energies between the C impurity and the surrounding Fe atoms in the GB is 8.84 eV/adatom, including the effects of the C-induced structural relaxation (which contributes only 0.16 eV to ΔE_b). On the other hand, the calculated ΔE_s is 8.23 eV/adatom, to which the C-induced structural relaxation contributes 0.36 eV/adatom. As a result, we obtain a negative free energy difference, i.e., $\Delta E_b-\Delta E_s=-0.61$ eV/adatom or 62 kJ/mole. Thus, the C impurity is a cohesive enhancer for the FeΣ3(111) grain boundary. Although there have been strong experimental indications that C is a cohesive enhancer, this is the first quantitative theoretical determination so far.

Finally, we can answer the question: what is the key factor determining the behavior of an impurity to the cohesive properties of the Fe GB—atomic size, number of electrons, or strength of hybridization? Since the value of $\Delta E_b-\Delta E_s$ is the key quantity, a comparison should be made to see the difference of these factors in the GB and FS environments. Combining the results here with those obtained previously for B/Fe and P/Fe,[10] it is obvious that the number of p electrons and the resulting spatial anisotropy (not the strength) of the bonding are the most significant factors. Of course, if the hybridization is weak (for larger atoms, e.g., Si and P, an embedded-atom like interaction is usually adopted[9]), the anisotropy of the bonding is also weak and thus the impurity tends to be an embritller.

TABLE III. Calculated Fe magnetic moments (in μ_B). GB0 and GB1 represent the relaxed and unrelaxed clean Fe GB, respectively.

Atom	Fe GB0	Fe GB1	C/Fe GB	Fe(111)	C/Fe(111)
Fe(1)	2.60	2.60	2.31	2.73	2.46
Fe(2)	1.90	1.92	2.20	2.20	2.32
Fe(3)	2.28	2.26	1.64	2.32	1.69
Fe(4)	2.19	2.18	2.43	2.15	2.41
Fe(5)	2.18	2.18	2.19	2.14	2.26
Fe(6)	2.14	2.11	2.30	2.11	2.39
Fe(7)	2.29	2.16	2.25	2.02	2.31

In the GB there are three Fe(1) and two Fe(3) atoms, while in the FS the three Fe(1) atoms are still present, but one of the Fe(3) atoms is missing. If the strength of the impurity-Fe(1) bonding is comparable to that of the impurity-Fe(3) bonding, only one out of five impurity-Fe bonds is cut from GB to FS. Therefore, the energy loss due to the fracture should be small and can be easily compensated through release of the lattice stress in the GB. In this case, a positive $\Delta E_b-\Delta E_s$ is expected and an impurity (such as P and S) is likely to be an embrittler. By contrast, if the impurity-Fe(1) bond is much weaker than that between impurity-Fe(3), one out of two bonds is cut in the fracture and it will be very hard to compensate the loss of energy. Of course, the GB environment is preferred for such an impurity [e.g., B (Ref. 23) and C], which then acts as a cohesive enhancer.

ACKNOWLEDGMENTS

Work supported by the Office of Naval Research (Grant No. N00014-90-J-1363) with seed funding from the National Science Foundation MRL program (Grant No. DMR88-16126 and a grant of Cray-C90 computer time at the Pittsburgh Supercomputing Center from its Division of Advanced Scientific Computing).

[1] G.B. Olson, in *Innovations in Ultrahigh-Strength Steel Technology*, edited by G.B. Olson, M. Azrin, and E.S. Wright, Sagamore Army Materials Research Conference Proceedings No. 34 (U.S. Army Laboratory Command, 1990), p. 3.

[2] J.R. Rice and J.-S. Wang, Mater. Sci. Eng. A **107**, 23 (1989).

[3] P.M. Anderson, J.-S. Wang, and J.R. Rice, in *Innovations in Ultrahigh-Strength Steel Technology* (Ref. 1), p. 619.

[4] In this notation, Σ3 refers to a special orientation relation between crystals for which one in three lattice points are coincident, $[1\bar{1}0]$ denotes the crystal Miller indices of the axis of misorientation, and (111) denotes the habit plane of the boundary, both referred to the body-centered cubic crystal lattice of Fe. The boundary corresponds to the ''incoherent'' twin boundary.

[5] C.L. Briant and R.P. Messmer, Philos. Mag. B **42**, 569 (1980); R.P. Messmer and C.L. Briant, Acta. Metall. **30**, 457 (1982).

[6] M.E. Eberhart and D.D. Vvedensky, Scr. Metall. **22**, 183 (1988); J.M. MacLaren, S. Crampin, D.D. Vvedensky, and M.E. Eberhart, Phys. Rev. Lett. **63**, 2586 (1989).

[7] G.L. Krasko and G.B. Olson, Solid State Commun. **76**, 247 (1990).

[8] R. Wu, A.J. Freeman, and G.B. Olson, J. Mater. Res. **7**, 2433 (1992).
[9] R. Wu, A.J. Freeman, and G.B. Olson, Phys. Rev. B **50**, 75 (1994).
[10] R. Wu, A.J. Freeman, and G.B. Olson, Science **265**, 376 (1994).
[11] E. Wimmer, H. Krakauer, M. Weinert, and A.J. Freeman, Phys. Rev. B **24**, 864 (1981), and references therein.
[12] S.P. Tang, A.J. Freeman, and G.B. Olson, Phys. Rev. B **47**, 2441 (1993).
[13] Defined as the first derivative of the total energy, with respect to the atomic position, the force calculated in the FLAPW approach contains both the Hellmann-Feynman term and the Pulay correction terms. R. Wu and A.J. Freeman will give a detailed discussion for the force evaluation elsewhere. Also, see papers by J.M. Soler and A.R. Williams, Phys. Rev. B **40**, 1560 (1989); R. Yu, D. Singh, and H. Krakauer, *ibid.* **43**, 6411 (1992).
[14] D.D. Koelling and B.N. Harmon, J. Phys. C **10**, 3107 (1977).
[15] U. von Barth and L. Hedin, J. Phys. C **5**, 1629 (1972).
[16] A.J. Freeman and R. Wu, J. Magn. Magn. Mater. **100**, 497 (1992).
[17] R. Wu and A.J. Freeman, Comput. Phys. Commun. **76**, 58 (1993).
[18] G.L. Krasko, in *Structure and Properties of Interfaces in Materials*, edited by W.A.T. Clark, U. Dahmen, and C.L. Briant, MRS Symposia Proceeding No. 238 (Materials Research Society, Pittsburgh, 1991), p. 481.
[19] R. Wu and A.J. Freeman, Phys. Rev. B **47**, 3904 (1993).
[20] J. Sokolov, F. Jona, and P.M. Marcus, Phys. Rev. B **33**, 1397 (1986).
[21] K.B. Hathaway, H.J.F. Jansen, and A.J. Freeman, Phys. Rev. B **31**, 7603 (1985); C.S. Wang, B.M. Klein, and H. Krakauer, Phys. Rev. Lett. **54**, 1852 (1985).
[22] R. Wu, A.J. Freeman, and G.B. Olson, Phys. Rev. B **47**, 6855 (1993).
[23] We reoptimized the structures with the FLAPW force approach for the B/Fe system giving $\Delta E_b - \Delta E_s \approx -1.07$ eV, which means B is a better cohesive enhancer than C.